Magnetic order in nanocrystalline Cr and suppression of antiferromagnetism in bcc Cr

M. R. Fitzsimmons
Los Alamos National Laboratory, Los Alamos, New Mexico 87545

J. A. Eastman
Argonne National Laboratory, Argonne, Illinois 60439

R. A. Robinson, A. C. Lawson, J. D. Thompson, and R. Movshovich
Los Alamos National Laboratory, Los Alamos, New Mexico 87545

J. Satti
Argonne National Laboratory, Argonne, Illinois 60439

Neutron-diffraction data and magnetization measurements of compacted nanophase Cr are presented. Two crystalline Cr phases were found, the majority phase having a bcc structure and the minority phase having an $A15$ structure. The 100 Bragg reflection seen in antiferromagnetically ordered coarse-grained bcc-Cr polycrystals was not observed in the nanocrystalline sample, suggesting that antiferromagnetism was suppressed in the bcc phase to at least 20 K. The suppression of antiferromagnetism may be due to small grain sizes, strain from grain boundaries or other defects, and/or concentrations of impurities, any of which may restrict the development of magnetic correlations in the bcc material. A magnetic diffraction peak corresponding to the 110 Bragg reflection of the Cr $A15$ lattice was observed at 20 K and was not observed at 149 or 300 K, suggesting that the minority phase of the nanocrystalline sample becomes antiferromagnetically ordered at very low temperatures. Consistent with this observation, susceptibility measurements at several temperatures indicate that magnetic correlations develop below 100 K, representing at least momentary short-ranged magnetic order in the nanocrystalline sample.

I. INTRODUCTION

Nanocrystalline materials are composed of ultrafine grains, typically a few nanometers in diameter. Since the grain sizes of these materials are small, most atoms are within one or two atomic jumps of a grain boundary; therefore, grain boundaries are expected to influence strongly the properties of compacted nanocrystalline materials. In addition to small grain sizes and large interface content, these materials are also severely deformed or strained.[1,2] Compacted nanocrystalline materials often contain a significant amount of open porosity, which for reactive materials such as Cr may result in significant surface contamination when samples are exposed to air. Any combination of these characteristics, which are found at extremes in nanocrystalline materials, may produce unique magnetic properties. For example, ferromagnetism in compacted nanocrystalline Ni (Ref. 3) and bcc Fe (Ref. 4) is suppressed to lower temperatures compared to the bulk. Small-angle neutron-scattering (SANS) measurements[5] of nanocrystalline bcc Fe suggest that interfacial regions in the material are either nonmagnetic or weakly magnetic. Recently, Haneda et al.[6] determined that loose powders of 8-nm-diam γ-Fe (fcc Fe) grains did not exhibit magnetic ordering down to 1.8 K. Previously, larger γ-Fe grains precipitated from solutions of Cu were found to be antiferromagnetic,[7,8] and fcc Fe grains precipitated from an Fe-Ni solution were found to be both antiferromagnetic and ferromagnetic.[9]

Haneda et al. have suggested that the lack of magnetic ordering in nanocrystalline γ-Fe when ordering had been observed in other fcc-Fe systems lends support to theoretical predictions[10,11] that the ground state of fcc Fe is very sensitive to atomic volume. This explanation cannot be entirely correct, since the lattice parameter (and therefore the atomic volume) of the nanometer-sized γ-Fe grains of Haneda et al.,[6] which did not magnetically order, is about 0.8% *larger* than that of the micrometer-sized γ-Fe grains of Abrahams, Guttman, and Kasper,[8] which exhibited magnetic ordering. Impurities in the precipitated grains and/or spatial limitations of the nanocrystalline γ-Fe particles may also play a role in determining whether order occurs. For example, the lattice parameter, structure, and size of clusters, which are typically even smaller than nanocrystalline grains, are predicted to be important parameters in determining whether magnetic ordering occurs in V (Ref. 12) and Cr.[13] Atoms in clusters, whose densities are less than the bulk, are expected to have nonzero magnetic moments. Yet in Stern-Gerlach measurements of Al, Cr, Pd, and V clusters, Douglass, Bucher, and Bloomfield[14] determined that atoms in these clusters had zero magnetic moments. Observations and predictions of changes in the magnetic properties and gross features of the magnetic structures of nanocrystalline materials and clusters, which at times are at odds with each other, partially motivate the present study of the magnetic structure of nanocrystalline Cr at the atomic scale.

In addition to scientific interest, there exists considerable technological motivation to study Cr, particularly from the magnetic recording industry. For example, the next generation of magnetic hard disks may utilize multilayer films, including thin films of Cr.[15] In this application, the Cr layer promotes the textured growth of a ferromagnetic overlayer with small grain size. Since grain boundaries hinder the growth of magnetic domains,[15] materials with small magnetic domains can be produced by growing the Cr film with a grain size that approaches the nanometer scale, thus leading to an increase of information that can be stored on the device. The utilization of a nanocrystalline Cr thin film as a substrate to grow the magnetic storage medium may be unsuccessful depending upon whether the magnetic properties of the Cr layer affect those of the medium. It is, therefore, important to determine the magnetic properties of nanocrystalline Cr.

Since Cr is the classic example of an itinerant antiferromagnet, its magnetic structures have been widely studied. Above the Néel temperature, $T_N = 311$ K, single-crystal Cr is paramagnetic.[16] Below T_N and above the spin-flip temperature $T_{SF} = 123$ K, single-crystal Cr is antiferromagnetic (AF) with a transversely polarized spin density wave (SDW) that propagates in the [100] direction and is incommensurate with the Cr nuclear lattice (the AF_1 phase).[16] Below T_{SF}, the SDW remains incommensurate, but becomes longitudinally polarized (the AF_2 phase).[16] In its polycrystalline form, Cr exhibits a combination of these three magnetic phases and a fourth magnetic phase[17]—a simple commensurate antiferromagnetic (AF_0) phase. Bacon and Cowlam[17] have shown that the occurrence of the various magnetic phases can be greatly altered by the introduction of strain into polycrystalline Cr. For example, the AF_1 phase is found *above* T_{SF} in single-crystal Cr, but is found *below* T_{SF} in heavily strained Cr polycrystals, and vice versa for the AF_2 phase.[17] The magnetic structures of Cr are also sensitive to alloying or concentrations of impurities.[16] For example, the AF_0 phase of Cr can be stabilized at room temperature through the addition of small amounts (<2 at. %) of Mn.[18] The incorporation of strain and/or impurities into nanocrystalline Cr may also affect its magnetic structure.

II. SPECIMEN PREPARATION

Nanocrystalline samples were prepared by evaporating high-purity Cr in 500 Pa of 99.9999% pure He to condense ultrafine crystalline particles in a vacuum chamber which had been previously evacuated to $\sim 10^{-5}$ Pa. The particles were then consolidated into disks at room temperature under vacuum conditions, following the procedures first suggested by Gleiter.[19] Typically, the disks had diameters of 9 mm and thicknesses ranging from 0.1 to 0.5 mm. Thirteen disks were produced, yielding about 1 g of compacted nanocrystalline Cr. The median grain size of the compacted disks, ~ 11 nm, was measured using transmission electron microscopy. The densities of the samples, which were determined from weight and volume measurements, fell within a range of $(52\pm10)\%$,

that of bulk Cr (7.19 g/cm^{-3}).[20] Some of the samples were also analyzed for the content of C, H, N, and O. The samples were found to contain 0.35 wt % H, 0.97 wt % C and 0.19 wt % N. Oxygen in the form of H_2O and CO_2 was found at a level of 0.07 wt %. A significant amount of O (6.9 wt % or about 19 at. %) was found in the samples in the form of CrO_x and/or $CrO_x H$.

III. DIFFRACTION AND MAGNETIZATION MEASUREMENTS

Neutron-diffraction measurements were made using the high-intensity powder diffractometer[21] (HIPD) at the Los Alamos Neutron Scattering Center (LANSCE). The diffraction observations with d spacing ranging from 0.35 to 6.3 Å were obtained from a 10-g sample of 99.999% pure coarse-grained Cr pieces at 20, 149, and 232 K. Portions of the measurements at 20 and 323 K in the neighborhood of the 100 magnetic Cr Bragg reflection are shown in Fig. 1(a) (●). Similar measurements of the nanocrystalline sample were made at temperatures of 20, 149, and 300 K and are shown in Fig. 1(b). Measurements at 20 K over a larger range of d spacing are shown in Fig. 2. Some of the diffraction peaks in the figure are indexed with respect to the reciprocal lattice coordinates of the bcc and A 15-Cr phases. The A 15 structure of Cr is identical to that of Cr_3O [isostructural with W_3O (or β-W) and having space group $Pm3n$],[22-24] and can be
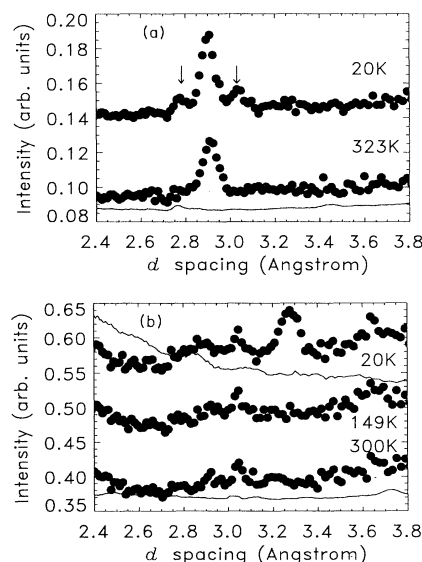

FIG. 1. (a) A portion of the neutron-diffraction patterns (●) at 20 and 323 K from coarse-grained Cr polycrystal pieces, and a portion of the x-ray diffraction pattern (solid curve) at 300 K from a coarse-grained Cr foil are shown. The central peaks in the neutron data are located at the position of the 100 Bragg reflection for bcc Cr. The arrows point to the satellite peaks about the magnetic reflection in the 20-K data. (b) A similar portion of the neutron-diffraction patterns (●) at 20, 149, and 323 K from the nanocrystalline Cr sample, and a portion of the x-ray diffraction patterns (solid curves) at 20 and 300 K taken from a representative portion of the sample used in the neutron experiment. The curves corresponding to different temperatures have been displaced for clarity.
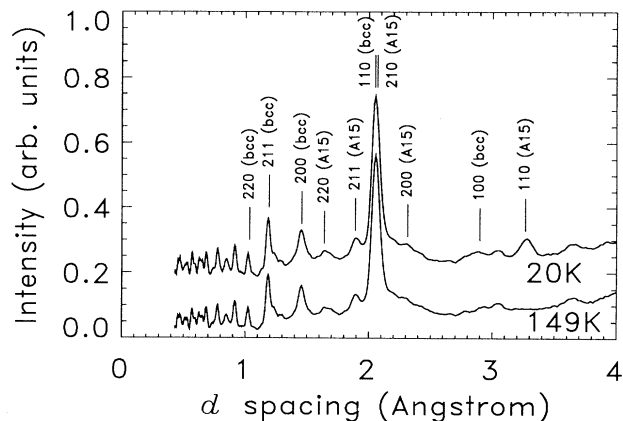
FIG. 2. A large portion of the neutron-diffraction patterns from the nanocrystalline sample taken at 20 and 149 K are shown with diffraction peaks marked.

FIG. 3. Depiction of the A 15 unit cell of Cr_3O with oxygen ($\bigcirc$) and Cr ($\bullet$) lattice sites marked. In the A 15-Cr phase the oxygen lattice sites are occupied by Cr atoms. The direction of the nonzero magnetic moments in the unit cell are shown with arrows. Cr atom sites hidden by the perspective are shaded.

thought of as Cr_3Cr with Cr atoms occupying oxygen sites. The oxygen atoms form a bcc lattice. The A 15 phase was not observed in the coarse-grained sample.

X-ray diffraction measurements corresponding to some of the neutron measurements are shown as the solid curves in Fig. 1. The x-ray data were scaled to enhance features in the diffraction pattern so that the x-ray intensity of the 110 bcc Bragg reflection from the coarse-grained sample was ten times larger than that measured with neutrons, which in turn was scaled to measurements of the nanocrystalline sample by the ratio of the sample weights.

Rietveld refinements of the neutron data, using the general structure analysis system (GSAS),[25] yielded information about the composition of the nanocrystalline sample. The neutron-diffraction peaks were satisfactorily represented by a combination of bcc-Cr, A 15-Cr, and vanadium crystalline phases. The vanadium phase was observed because the can used to contain the sample was made from vanadium. From the GSAS analysis, 85 wt % of the crystalline portion of the sample was found to be nanocrystalline bcc Cr, while the remaining 15 wt % crystalline portion was determined to have the A 15-Cr structure. The unit cell of the A 15 structure has cubic symmetry ($a_0 = 4.5759 \pm 0.0001$ Å) with Cr atoms occupying oxygen lattice sites ($\bigcirc$) and pairs of Cr atoms ($\bullet$) on each cube face, as shown in Fig. 3. The A 15 Cr phase has also been observed in coarse-grained Cr powders by Shönberg[22] and in loose nanocrystalline Cr powders by Kimoto and Nishida.[26] If the formation of the A 15-Cr structure is similar to that of β-W, then only very small amounts of oxygen need to be present on the oxygen lattice (with the remaining sites occupied by W or Cr in the case of β-W or A 15-Cr, respectively[23,24]) in order to stabilize the A 15 structure.

The chemical composition of the A 15 phase is believed to be nearly Cr_3Cr rather than Cr_3O, since the 110 reflection from the A 15 structure is absent in the diffraction patterns taken at 149 and 300 K. The absence of this reflection occurs when the scattering amplitude from atoms on oxygen lattice sites negates that of Cr atoms on Cr sites. The destructive interference is only
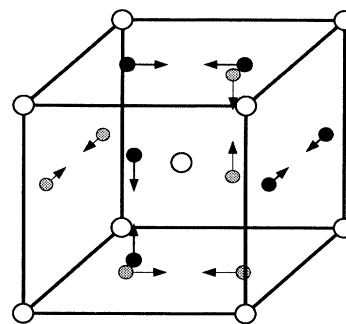
possible when the scattering length (x ray or neutron) of the atoms on oxygen sites is the same as Cr.

The GSAS analysis also yielded information about the microstructure of the bcc portion of the nanocrystalline sample, e.g., strain and particle size distributions of the grains. The values of the root-mean-square magnitudes of microstrain broadening (strain distribution width) σ_ϵ, and particle size distribution P, and the lattice and Debye-Waller parameters a_0 and B, respectively, of the bcc Cr portion of the nanocrystalline sample are shown in Table I. The lattice parameter of nanocrystalline bcc Cr does not differ significantly from that of the coarse-grained sample.

Diffraction peaks in the x-ray and neutron data were superimposed on a substantial background.[27] The form of the background was characteristic of scattering from an amorphous material. This material might be composed of amorphous chromium oxide, e.g., CrO_2 or Cr_2O_3, phases, since 6.9 wt % of the entire sample was determined from chemical analysis to be chromium oxide. Considering the details of the manufacturing process and the porosity of the nanocrystalline samples (52% dense), chromium oxide may have formed and surrounded individual crystalline Cr grains after exposure of the samples to air following powder consolidation. This hypothesis can be tested in future SANS experiments, since the scattering length of a chromium oxide phase boundary is different than a pure Cr grain. Alternatively, the surface area available for oxygen contamination might be reduced if denser samples can be manufactured.

The magnetization density M of an 8.9-mg portion of the nanocrystalline sample was measured versus applied

TABLE I. Parameters of the Rietveld refinement.

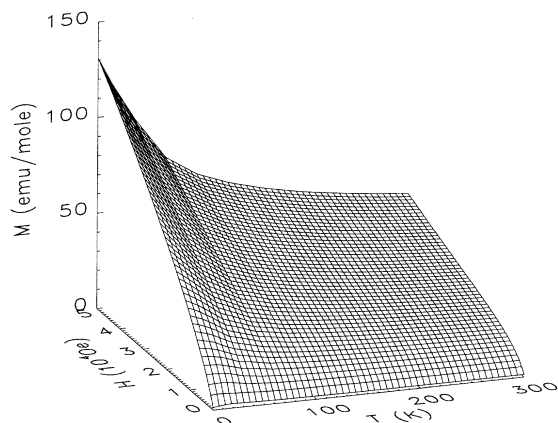| Parameter	Nanosample	Coarse-grained sample
σ_ϵ (%)	1.0 ± 0.1	0.7 ± 0.1
P (nm)	11.0 ± 1.0	
$a_0(323$ K) (Å)	2.887 ± 0.001	2.886 ± 0.001
$a_0(20$ K) (Å)	2.883 ± 0.001	2.882 ± 0.001
$B(323$ K) (Å^2)	0.59 ± 0.01	0.27 ± 0.01
$B(20$ K) (Å^2)	0.46 ± 0.01	0.11 ± 0.01

FIG. 4. The magnetization densities (M) of a representative portion of the nanocrystalline Cr sample for several temperatures (T) and applied magnetic fields (H).

magnetic field H using a SQUID magnetometer at several temperatures T (Fig. 4). These data exhibit a Curie-Weiss-type variation of the magnetization density superimposed upon that typical of a ferromagnet which becomes saturated when $H > 10^4$ Oe. The raw data were measured in units of emu, and have been converted by the factor 1.7×10^{-4} to units of emu/mole in Fig. 4 under the assumption that the entire sample was Cr.

IV. DISCUSSION

A. Microstructure analysis

Since the majority of the nanocrystalline sample was composed of bcc-Cr grains, the analysis of the microstructure of the nanocrystalline sample will be made considering only this phase. Both the coarse-grained sample and the bcc portion of the nanocrystalline sample showed significant microstrain broadening, 0.7% and 1.%, respectively. Microstrain broadening is produced by linear defects such as dislocations or planar defects such as grain boundaries, twins, or stacking faults, whose strain fields decay more slowly than $1/r^{3/2}$, where r is the distance from the defect.[28] These defects may be located within crystalline grains and/or at interfaces. Large distributions of microstrain broadening have been observed in other nanocrystalline systems, specifically Pd (Refs. 1 and 2) and Dy.[29]

Strain in a material may also be generated by point defects or dislocation loops. Since strain from point defects and dislocation loops decays more quickly than $1/r^{3/2}$, these defects attenuate the intensities of Bragg reflections and this strain is manifested as a static Debye-Waller parameter.[28] In general, the observed attenuation is a combination of static and thermal Debye-Waller parameters. The total Debye-Waller parameter of the nanocrystalline Cr sample was found to be greater than that of the coarse-grained sample at all temperatures (see Table I). Since the changes in the Debye-Waller parameters from 20 K to room temperature are the same in the two samples, the thermal mean-square displacements of atoms in

bulk Cr and the bcc portion of the nanocrystalline material are the same. The difference between the Debye-Waller parameters at each temperature, ~ 0.35 Å^2, is an indication that the nanocrystalline Cr sample contains many more defects with short-ranged strain than the coarse-grained material. Similar conclusions were made by Eastman, Fitzsimmons, and Thompson,[2] in a study of the thermal properties of nanocrystalline and coarse-grained Pd.

Based upon observations of significant particle size and microstrain broadening of diffraction peaks, attenuation of these peaks due to static displacements, and scattering from incoherent sources, the microstructure of nanocrystalline Cr can be described as a collection of mostly small crystalline bcc grains, which are severely distorted by point, linear, and/or planar defects, surrounded by grain or phase, i.e., chromium oxide, boundaries. The coherent structures of grain or phase boundaries may be distorted by point and linear defects. Alternatively, the attenuation and strain broadening of diffraction peaks may result from combinations of strains, e.g., those which decay relatively quickly away from boundaries that surround very small crystals (appearing more "pointlike"), and those which slowly decay away from nearly planar boundaries that might surround large grains. Regardless of their sources, severe distortions in nanocrystalline materials may have important consequences on their magnetic structure and properties, since the distortions introduced by cold-working, e.g., dislocations,[30] alter the magnetic properties of Cr polycrystals.[17]

Since the width of the 211 reflection from the A15-Cr phase is similar to that of the 110 reflection from the bcc phase, and the former reflection does not coincide with a reflection from any other phase in the sample, the size distribution of the A15-Cr grains is probably similar to that of the bcc component. Unfortunately, the lack of diffraction intensity from this phase makes a determination of its strain content unreliable. In light of the fact that 85% of the crystalline sample is severely strained, it is reasonable to expect that the A15-Cr phase is also severely strained.

B. Magnetic structure of coarse-grained Cr

Since the spin of a neutron can couple to the magnetic moment of an atom, neutron diffraction can also be used to determine the magnetic structures of materials. In a simple antiferromagnet, the magnetic moments of atoms in adjacent planes may be ordered antiparallel to one another. In this example, the lattice parameter of the magnetic lattice is twice the size of the atomic lattice; thus Bragg reflections from the magnetic lattice are observed at positions of reflections forbidden by the atomic lattice. This is qualitatively the reason for the occurrence of a diffraction peak at the 100 reciprocal lattice coordinate of bcc-Cr, which is shown in Fig. 1(a) for the coarse-grained sample. Since the magnetic and nuclear scattering lengths of neutrons are generally similar, e.g., the nuclear and magnetic scattering lengths of Cr are 0.35×10^{-12} and 0.11×10^{-12} cm (using the literature value of the rms magnetic moment of Cr,

$\mu = 0.43\mu_B$),[31-33] respectively, while the magnetic scattering length of x rays is negligible, the magnetic 100 reflection in the neutron diffraction pattern should not appear in the x-ray diffraction pattern. The absence of an x-ray peak at the 100 bcc reflection, when even weaker features relative to the 110 bcc Bragg reflection, e.g., at $d = 2.77$ and 3.43 Å, are observed, suggests that the 100 bcc Bragg reflection (and its satellites) in the neutron-diffraction pattern of the coarse-grained sample have magnetic origins.

The central peak at $d_{100} = 2.884$ Å, corresponding to the 100 Bragg reflection, in the 20-K data from the coarse-grained sample [Fig. 1(a)], is accompanied by two satellite peaks. The positions of the satellites (d spacings of 2.768 and 3.017 Å) can be used to determine the magnitude of the spin density wave vector $Q_{SDW} = (2\pi/d_{100})(1\pm\delta)$, where $\delta = 0.04$. This value is in good agreement with those reported for the AF_1 phase of polycrystalline Cr below T_{SF} (Ref. 17) and in single-crystal Cr above T_{SF}.[16] The single peak observed at 323 K (12 K above T_N for single-crystal Cr) is consistent with observations of the AF_0 phase in Cr polycrystals at similar temperatures above T_N.[17]

The second magnetic reflection of bcc Cr is the 111 reflection ($d_{111} = 1.666$ Å). This reflection was not observed in the present experiment. When the multiplicities, and the magnetic form[16] and Lorentz-polarization factors of the 100 and 110 reflections (with respect to the bcc lattice) are considered, the intensity of the 111 reflection is expected to be 17 times weaker than that of the 100 reflection. The intensity of the 111 reflection is more than an order of magnitude weaker than that which can be reliably detected using the HIPD for the size of the coarse-grained sample; therefore, the 111 reflection is not expected to appear in the neutron-diffraction pattern. Nevertheless, the consistency between the observations of the 100 bcc reflection and reports in the literature[16,17] demonstrates that the HIPD is well suited to the study of antiferromagnetic ordering in Cr (at least for $d > 2$ Å), and should detect antiferromagnetic ordering (if it occurs) in nanocrystalline Cr.

C. Magnetic ordering and its suppression in nanocrystalline Cr

A peak at $d = 3.257$ Å with an integrated intensity equal to the strongest magnetic reflection in Fig. 1(a) is observed in the data taken at 20 K from the nanocrystalline sample [Figs. 1(b) and 2]. Since this peak is not observed in the x-ray diffraction pattern, its origin is likely due to antiferromagnetic ordering. The disappearance of the peak in the data taken at 149 and 300 K suggests that the nanocrystalline material, specifically the portion of the sample that was antiferromagnetic at 20 K, becomes paramagnetic (or loses long-ranged magnetic order) at some temperature between 20 and 149 K. In addition to the magnetic reflection, very weak peaks at $d = 3.02$ and 3.65 Å are observed at all temperatures in the neutron-diffraction pattern from the nanocrystalline sample [see Fig. 1(b)]. Since these peaks are also observed in the x-ray diffraction pattern at room temperature, they do not

have magnetic origins. Their origins have not yet been identified.

The position of the magnetic reflection corresponds to within 0.04% of location of the 110 Bragg reflection from $A15$-Cr. The position of this reflection is not consistent with that of a reflection from antiferromagnetic bcc Cr (even the location of a $\frac{1}{2}\frac{1}{2}\frac{1}{2}$ superlattice reflection, should it exist, is more than 2% different from that of the observed peak), any chromium oxide nuclear phase, or antiferromagnetic Cr_2O_3. Since the 110 reflection from $A15$-Cr is forbidden in the absence of antiferromagnetic ordering, the nonzero intensity of this reflection at 20 K suggests that the scattering lengths of Cr atoms on oxygen and Cr sites are different. This difference can be accounted for if the magnetic moments of the two atoms on the two sites are different. Since only one magnetic reflection is observed for d spacings greater than 2 Å, the magnetic structure of $A15$-Cr may have a high degree of symmetry. If the magnetic structure is to retain the cubic symmetry of the $A15$ atomic lattice, then magnetic space group analysis can be used to show that only one magnetic structure is possible. The cubic symmetry of the magnetic structure (space group $Pm3n'$) requires that Cr atoms on oxygen sites (open circles in Fig. 3) have zero magnetic moment while the magnetic moments of pairs of Cr atoms on Cr sites (solid circles in Fig. 3) are nonzero and lie in opposing directions as shown by the arrows in Fig. 3. Refinements of this model to the data, using GSAS, indicate that the magnetic moment of a Cr atom on a Cr site has magnitude $(2.5\pm0.2)\mu_B$. This value is considerably larger than the value of $0.62\mu_B$ found in the literature[33] for bulk (bcc) Cr, but is comparable to the magnetic moments of Cr atoms in chromium oxide, e.g., CrO_2 ($2.03\mu_B$) (Ref. 34) and Cr_2O_3 ($3.73\mu_B$).[35]

Noteworthy by its absence in the neutron-diffraction patterns at all temperatures is the 100 bcc magnetic reflection from the nanocrystalline sample. As demonstrated by the neutron measurements of the coarse-grained sample, the 100 bcc reflection should have been observed in the nanocrystalline sample if the bcc phase of the sample was antiferromagnetically ordered. Since this reflection was not observed, antiferromagnetism in the bcc portion of the nanocrystalline sample is suppressed, if it occurs at all, to below 20 K.

D. The magnetization and susceptibility of nanocrystalline Cr

Since CrO_2 is ferromagnetic below 394 K,[34] and chemical analysis of the nanocrystalline sample detected chromium oxide, CrO_2 may be responsible for the component of the magnetization curve which saturates in applied magnetic fields greater than 10^4 Oe. By extrapolating the fit of the Curie-Weiss law in the high-field region to zero field, the magnetization of the saturated portion of the sample can be determined. The zero-field value was consistently found to be 0.0018 emu (in units the raw data were acquired) at all temperatures. From this value, and using the literature values of the saturation magnetization and density of CrO_2 [490 emu/cm^3 (Ref. 36) and 4.89 g/cm^3,[37] respectively], the fraction of CrO_2 in the

sample is calculated to be 0.2 wt %. This fraction is considerably less than the 6.9 wt % of chromium oxide in the nanocrystalline sample reported by chemical analysis. The difference in weight fractions might be accounted for by a nonferromagnetic amorphous oxide phase, e.g., Cr_2O_3.

The molar magnetic susceptibility χ_m of the nonferromagnetic portion of the nanocrystalline sample, including (although not necessarily exclusively so) the portion of the sample contributing to the magnetic reflection, can be calculated from the slope of the linear portion of the magnetization curves in the region where $H > 10^4$ Oe. In this region, the ferromagnetic component is saturated so it does not contribute to the differential magnetic susceptibility. A plot of the inverse molar susceptibilities χ_m^{-1} as a function of temperature is shown in Fig. 5. The increase of χ_m^{-1} from 150 to 300 K is consistent with the variation of χ_m^{-1} for a paramagnetic material and the conclusion from the neutron measurements that a portion of the nanocrystalline material is paramagnetic when $T \geq 149$ K, since no magnetic reflection was observed in this temperature range. Fitting the Curie-Weiss law to the increase of χ_m^{-1}, the effective magnetic moment μ_{eff} is calculated to be $(1.8\pm0.1)\mu_B$.

Since the SQUID magnetometer measures the magnetization of the entire sample, the value of μ_{eff} represents a weighted average of the magnetic moments of the different phases in the sample. For example, the susceptibility of a chromium oxide, e.g., Cr_2O_3—an antiferromagnet below 340 K,[36] might increase with increasing temperature from 150 to 300 K (behavior typical of an antiferromagnet). In the same temperature region, the susceptibility of the nanometer-sized crystalline bcc and A 15-Cr grains, which are both paramagnetic above 149 K (no magnetic reflection is observed in the neutron-diffraction pattern), might exhibit a Curie-Weiss temperature dependence, i.e., a decrease in the susceptibility with increasing temperature. The observed susceptibility of the nanocrystalline sample would then be a weighted average of the susceptibilities from an antiferromagnetic chromium oxide and paramagnetic nanometer-sized crystalline Cr grains. If this scenario were correct, then the temperature dependence of the susceptibility of nanometer-sized crystalline Cr grains would be substan-

tially different from that of the coarse-grained material, which does not exhibit Curie-Weiss temperature dependence as a paramagnet.[38]

If the nanocrystalline sample were composed of localized magnetic moments, then μ_{eff}, which is proportional to $g\sqrt{J(J+1)}$,[31] where g is the Landé splitting factor and J is the total angular momentum of the magnetic atom, would represent a significant increase of 290% over the magnetic moment of antiferromagnetic Cr in the bulk, $\mu_0 = 0.62\mu_B = \sqrt{2}\mu$ [which unlike μ_{eff} is proportional to gJ (Ref. 31)].[32,33] Since pure bcc-Cr is an itinerant antiferromagnet, this comparison is inappropriate. However, the magnitude of μ_{eff} may be partly due to impurities in portions of the sample other than the bcc phase, e.g., the A 15-Cr or amorphous chromium oxide phases. Impurities (presumably the A 15-Cr phase, like β-W,[23,24] is stabilized by small quantities of oxygen) may alter the magnetic behavior of Cr from that of an itinerant magnet to that of a collection of localized moments such as found in the chromium salts.[39]

The deviation of χ_m^{-1} from a linear extrapolation of the variation of χ_m^{-1} in the paramagnetic region, i.e, below 100 K, is an indication that magnetic correlations develop in the material at low temperatures. The term "magnetic correlations" refers to spatially limited regions of the sample which exhibit magnetic order for possibly short periods of time. Evidence for magnetic correlations at low temperatures is consistent with neutron-diffraction evidence for antiferromagnetic ordering at 20 K in the A 15-Cr portion of the nanocrystalline sample, since antiferromagnetic order is one form of magnetic correlation. If the magnetic correlations indicated by the susceptibility measurements are a consequence of antiferromagnetic ordering, then the Néel temperature of the A 15-Cr portion of the nanocrystalline sample studied in the present work can be tentatively given as 100 K. Not all samples may exhibit the same T_N. For example, if the depression of T_N to low temperatures is caused by small grain sizes, strain, and/or impurities, then samples produced under different conditions may exhibit different Néel temperatures. In the future, the Néel temperature of A 15-Cr might be determined by observing the temperature dependence of its magnetic reflection with neutron diffraction between 20 and 149 K.
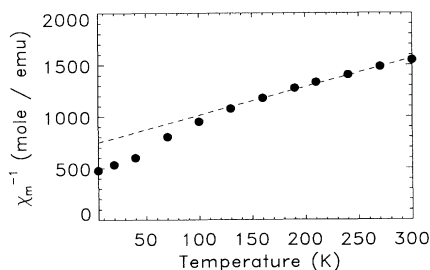
E. Suppression and origin of magnetic ordering in nanocrystalline Cr

The suppression of antiferromagnetism in nanocrystalline bcc-Cr may be a consequence of the spatial limitations imposed upon the crystalline grains by the high density of grain or phase boundaries. This spatial limitation may hinder the development in the material of magnetic correlations, which are necessary for magnetic ordering to occur. Alternatively, the severely deformed state of the nanocrystalline sample may also hinder magnetic ordering, since strain in polycrystalline Cr can profoundly change its magnetic structure. For example, the bcc portion of the nanocrystalline sample is known to be

FIG. 5. The variation of the inverse molar susceptibility χ_m^{-1} of a representative portion of the nanocrystalline Cr sample vs temperature.

severely strained, yet the mean lattice parameter of this portion is also known to be the same as the coarse-grained material; therefore, regions of the bcc material must be locally expanded (lattice parameter larger than the bulk) while other regions are locally contracted (lattice parameter smaller than the bulk). Several theoretical calculations have shown that $3d$ transition elements are magnetic when they exist as free atoms, but can become nonmagnetic when they form solid materials. The suppression of the magnetic moments of even ferromagnetic transition materials has been predicted when their densities are increased from bulk values; therefore, magnetism may be suppressed in regions of the nanocrystalline bcc-Cr material where its lattice parameter is locally smaller than the bulk material. Conversely, atoms in regions of the material where the lattice parameter is locally expanded may have magnetic moments yet are so confined by the nonmagnetic regions that magnetic order is suppressed. Since grain boundaries are typically regions that are locally expanded,[40,41] the magnetic moments of atoms in these regions may be enhanced compared to the bulk yet their magnetic ordering may be difficult in light of the fact that grain boundaries are spatially limited [~ 10 Å thick (Refs. 40 and 41)] and have reduced symmetry compared to the bulk.[40,41] If the grain boundaries in the nanocrystalline sample are locally expanded, then the interior of the nanocrystalline bcc-Cr grains is expected to be somewhat more dense than the bulk; consequently, the magnetic moments of atoms in the grains might be reduced as found to be the case for atoms in Cr clusters.[14]

Presumably, the A 15-Cr portion of the sample is also spatially limited and severely strained, so one is led to ask the following: Why would this material be magnetically ordered when the bcc phase is not? The answer may lie in the nature of the magnetism in the two phases. Whereas bcc-Cr is known to be an itinerant magnet, i.e., its magnetic properties are derived from its band structure, the magnetic properties of A 15-Cr, which are not known, may be better described by a collection of localized magnetic moments that may be less affected by spatial limitations or strain than those of an itinerant magnet. This hypothesis can be tested when pure samples of nanocrystalline bcc-Cr and A 15-Cr are obtained.

In 1972, Schmidt et al.[42] observed superconductivity in thin films of Cr deposited on a substrate with ion-beam sputtering. The transition temperatures T_c for superconductivity depended upon the ion species used in the sputtering process. For example, T_c was measured to be 1.52 K when a Xe ion beam was used to deposit the Cr, while T_c was 0.96 K for films deposited with a Kr ion beam.[42] The observation of superconductivity in Cr is very unusual, since magnetically ordered metals do not normally exhibit superconductivity.[43] One explanation for the observation is that the Xe and Kr incorporated into their films during the deposition were actually the superconducting component and not Cr. Interestingly, Schmidt et al. determined with x-ray diffraction the crystal structure of the Cr films to be bcc with a grain size of ~ 12 nm. The grain size of their films is very similar to the grain size of the nanocrystalline sample (~ 11 nm)

studied in the present work, where antiferromagnetism was suppressed in the bcc phase to at least 20 K. If antiferromagnetism was also suppressed in the Cr thin films of Schmidt et al., then their observation of superconductivity in Cr may not be so surprising. Their observation motivated a resistance measurement of the nanocrystalline sample studied in the present work and no superconductivity of the specimen was detected to 50 mK. The lack of superconductivity in the present specimen may be a consequence of its impurity content or perhaps the entire specimen is magnetically ordered below 20 K, thus preventing superconductivity. Clearly, purer samples are required before the existence of superconductivity in nanocrystalline Cr can be determined.

V. CONCLUSIONS

No evidence for antiferromagnetic ordering of nanometer-sized-crystalline grains of bcc-Cr was observed in neutron-diffraction data taken at temperatures as low as 20 K. The suppression of antiferromagnetism in bcc-Cr may result from spatial limitations imposed upon the ultrafine grains which hinder the development of magnetic correlations. Alternatively, magnetic ordering in the bcc portion of the sample may be hindered by the severely deformed microstructures of the nanocrystalline material.

Antiferromagnetic ordering, however, was observed in a portion of the nanocrystalline sample with the A 15 structure of Cr at 20 K. The ordering phenomenon was identified by noting the disappearance of a neutron diffraction peak at $d = 3.257$ Å, corresponding to the 110 Bragg reflection from A 15-Cr, when the temperature of the sample was raised above 20 K, and the absence of this reflection at any temperature in the x-ray diffraction data. The position of the peak is not consistent with the positions of magnetic reflections from bcc-Cr or antiferromagnetic chromium oxide phases, which in any case, are not observed as crystalline phases.

Magnetization measurements suggest that a portion (about 0.2 wt %) of the nanocrystalline sample is ferromagnetic at and below room temperature. The ferromagnetic material is likely to be amorphous CrO_2, since this material is known to be ferromagnetic in the bulk below 394 K, chromium oxide was detected in the nanocrystalline sample by chemical analysis, and amorphous material is suspected to be in the sample from the intensity of the incoherent background to the x-ray and neutron-diffraction patterns.

A significant deviation of the inverse molar susceptibility from a linear extrapolation of the values measured between 150 and 300 K, where most of the material appears to be paramagnetic, suggests that magnetic correlations develop in the nanocrystalline sample below 100 K in addition to the small ferromagnetic component that is observed at all temperatures. This conclusion is consistent with the neutron observation at 20 K of a magnetic reflection indicating long-ranged magnetic order, which is not seen at 149 or 300 K.

ACKNOWLEDGMENTS

[1] M. R. Fitzsimmons, J. A. Eastman, M. Müller-Stach, and G. Wallner, Phys. Rev. B **44**, 2452 (1991).

[2] J. A. Eastman, M. R. Fitzsimmons, and L. J. Thompson, Philos. Mag. B **66**, 667 (1992).

[3] H. E. Schaefer, H. Kisker, H. Kronmüller, and R. Würschum (unpublished).

[4] U. Herr, J. Jing, R. Birringer, U. Gonser, and H. Gleiter, Appl. Phys. Lett. **50**, 472 (1987).

[5] W. Wagner, A. Wiedenmann, W. Petry, A. Geibel, and H. Gleiter, J. Mater. Res. **6**, 2305 (1991).

[6] K. Haneda, Z. X. Zhou, A. H. Morrish, T. Majima, and T. Miyahara, Phys. Rev. B **46**, 13 832 (1992).

[7] U. Gonser, C. J. Meechan, A. H. Muir, and H. J. Wiedersich, J. Appl. Phys. **34**, 2373 (1963).

[8] S. C. Abrahams, L. Guttman, and J. S. Kasper, Phys. Rev. **127**, 2052 (1962).

[9] D. G. Rancourt, S. Chehab, and G. Lamarche, J. Magn. Magn. Mater. **78**, 129 (1989).

[10] D. Bagayoko and J. Callaway, Phys. Rev. B **28**, 5419 (1983).

[11] F. J. Pinski, J. Staunton, B. L. Gyorffy, D. D. Johnson, and G. M. Stocks, Phys. Rev. Lett. **56**, 2096 (1986).

[12] F. Liu, S. N. Khanna, and P. Jena, Phys. Rev. B **43**, 8179 (1991).

[13] G. M. Pastor, J. Dorantes-Dávila, and K. H. Bennemann, Phys. Rev. B **40**, 7642 (1989).

[14] D. C. Douglass, J. P. Bucher, and L. A. Bloomfield, Phys. Rev. B **45**, 6341 (1992).

[15] L. M. Falicov, D. T. Pierce, S. D. Bader, R. Gronsky, K. B. Hathaway, H. J. Hopster, H. N. Lambeth, S. S. P. Parkin, G. Prinz, M. B. Salamon, I. K. Schuller, and R. H. Victora, J. Mater. Res. **5**, 1299 (1990).

[16] E. Fawcett, Rev. Mod. Phys. **60**, 209 (1988).

[17] G. E. Bacon and N. Cowlam, J. Phys. C Ser. 2 **2**, 238 (1969).

[18] W. C. Koehler, R. Moon, A. L. Trego, and A. R. MacKintosh, Phys. Rev. **151**, 405 (1966).

[19] H. Gleiter, in *Deformation of Polycrystals: Mechanisms and Microstructures,* edited by N. Hansen *et al.* (Riso National Laboratory, Roskilde, 1981), p. 15.

[20] *International Tables for X-Ray Crystallography III,* edited by C. H. Macgillavry and G. D. Rieck (Reidel, Dordrecht, 1983).

[21] A. C. Lawson, J. A. Goldstone, J. G. Huber, A. L. Giorgi, J. W. Conant, A. Severing, B. Cort, and R. A. Robinson, J. Appl. Phys. **69**, 5112 (1991).

[22] N. Schönberg, Acta Chem. Scand. **8**, 221 (1954).

[23] G. Häag and N. Schönberg, Acta Crystallogr. **7**, 351 (1954).

[24] M. G. Charlton and G. L. Davis, Nature **175**, 131 (1955).

[25] A. C. Larson and R. B. Von Dreele, Los Alamos National Laboratory Report No. LA-UR-86-748, 1986 (unpublished).

[26] K. Kimoto and I. Nishida, J. Phys. Soc. Jpn. **22**, 744 (1967).

[27] In the absence of Lorentzian-shaped peaks, which contain a significant fraction of intensity in the wings of the peak, the intensity between peaks can be identified as background and/or diffusely scattered radiation. Since nanocrystalline materials usually produce Lorentzian-shaped peaks (Refs. 1 and 2), a careful analysis of the diffraction data is required to determine whether or not the apparent background is actually a combination of intensity from the wings of Lorentzian-shaped peaks with sources of background radiation. From the GSAS analysis used in the present study, background and/or diffusely scattered radiation from the nanocrystalline sample was determined to be more intense than that from the coarse-grained reference sample.

[28] M. A. Krivoglaz, *Theory of X-Ray and Thermal-Neutron Scattering by Real Crystals* (Plenum, New York, 1969).

[29] M. R. Fitzsimmons, J. A. Eastman, G. H. Kwei, J. D. Thompson, and L. J. Thompson (unpublished).

[30] B. E. Warren and B. L. Averbach, J. Appl. Phys. **21**, 595 (1950).

[31] G. E. Bacon, *Neutron Diffraction* (Clarendon, Oxford, 1975).

[32] A. Arrott, S. A. Werner, and H. Kendrick, Phys. Rev. Lett. **14**, 1022 (1965).

[33] G. Shirane, Acta Crystallogr. **12**, 282 (1959).

[34] C. Kittel, *Introduction to Solid State Physics,* 3rd ed. (Wiley, New York, 1967), p. 461.

[35] R. S. Tebble and D. J. Craik, *Magnetic Materials* (Wiley-Interscience, New York, 1969), p. 355.

[36] R. S. Tebble and D. J. Craik, *Magnetic Materials* (Ref. 35), pp. 155–161.

[37] *Crystal Data Determinative Tables,* 2nd ed., edited by J. D. H. Donnay, G. Donnay, E. G. Cox, O. Kennard, and M. V. King (American Crystallographic Association, Washington, D.C., 1963), p. 552.

[38] C. Kittel, *Introduction to Solid State Physics,* 5th ed. (Wiley, New York, 1976), p. 452.

[39] *American Institute of Physics Handbook,* 2nd ed., edited by D. E. Gray *et al.* (McGraw-Hill, New York, 1963), pp. 5-200 and 5-221.

[40] M. R. Fitzsimmons and S. L. Sass, Acta. Metall. **36**, 3103 (1988).

[41] M. R. Fitzsimmons and S. L. Sass, Acta. Metall. **37**, 1009 (1989).

[42] P. H. Schmidt, R. N. Castellano, H. Barz, B. T. Matthias, J. G. Huber, and W. A. Fertig, Phys. Lett. **41A**, 367 (1972).

[43] N. W. Ashcroft and N. D. Mermin, *Solid State Physics* (Holt, Rinehart and Winston, New York, 1976), p. 726